

Nonlinear Output Feedback Control of Underwater Vehicle Propellers using Feedback from Estimated Axial Flow Velocity

Thor I. Fossen, *Member, IEEE* and Mogens Blanke, *Senior Member, IEEE*

Abstract— Accurate propeller shaft speed controllers can be designed by using nonlinear control theory and feedback from the axial water velocity in the propeller disc. In this paper, an output feedback controller is derived, reconstructing the axial flow velocity from vehicle speed measurements, using a three-state model of propeller shaft speed, forward (surge) speed of the vehicle and the axial flow velocity. Lyapunov stability theory is used to prove that a nonlinear observer combined with an output feedback integral controller provide exponential stability. The output feedback controller compensates for variations in thrust due to time-variations in advance speed. This is a major problem when applying conventional vehicle-propeller control systems. The proposed controller is simulated for an underwater vehicle equipped with a single propeller. The simulations demonstrate that the axial water velocity can be estimated with good accuracy. In addition, the output feedback integral controller shows superior performance and robustness compared to a conventional shaft speed controller.

Keywords— Output feedback control, propeller shaft speed control, nonlinear control, underwater vehicles.

NOMENCLATURE

| | |
|------------|--|
| u | Surge speed of vehicle (m/s) |
| u_p | Axial flow velocity in propeller disc (m/s) |
| u_a | Ambient water velocity (advance speed) (m/s) |
| n | Propeller shaft speed (rad/s) |
| X_u | Linear damping coefficient in surge (kg/s) |
| $X_{u u }$ | Quadratic damping coefficient in surge (kg/m) |
| X_i | Added mass in surge (kg) |
| t | Thrust deduction number (-) |
| w | Wake fraction number (-) |
| m_f | Mass of water in propeller control volume (kg) |
| d_{f0} | Linear damping coeff. for control volume (kg/s) |
| d_f | Quadratic damp. coeff. for control volume (kg/m) |
| K_n | Linear motor damping coefficient (kgm ² /s) |
| $K_{n n }$ | Nonlinear motor damping coefficient (kgm ²) |
| J_m | Moment of inertia for DC-motor/propeller (kgm ²) |
| V_m | DC motor armature voltage (Volt) |
| i_m | DC-motor armature current (A) |
| τ | DC-motor control input (current, voltage or torque) |
| m | Mass of underwater vehicle (kg) |
| C_d | Drag coefficient (-) |
| D | Propeller diameter (m) |

| | |
|----------------------|---|
| T | Propeller thrust (N) |
| Q | Propeller torque (Nm) |
| J_0 | Advance ratio (-) |
| K_T | Thrust coefficient (-) |
| K_Q | Torque coefficient (-) |
| ρ | Density of water (kg/m ³) |
| ω_f | Natural frequency (rad/s) |
| α_1, α_2 | Thrust constants (-) |
| β_1, β_2 | Torque constants (-) |
| $T_{n n }$ | Thrust coefficient (kgm) |
| $T_{ n u_a}$ | Thrust coefficient (kg) |
| $Q_{n n }$ | Torque coefficient (kgm ²) |
| $Q_{ n u_a}$ | Torque coefficient (kgm) |
| Q_0 | Torque due to shaft speed (Nm) |
| Q_1 | Torque due to axial flow velocity (Nm) |
| T_0 | Thrust due to shaft speed (N) |
| T_1 | Thrust due to axial flow velocity (N) |
| A_{surge} | Cross-sectional area in surge (m ²) |
| A_p | Propeller disc area (m ²) |

I. INTRODUCTION

UNMANNED underwater vehicle (UUV) speed and position control systems are subject to an increased focus with respect to performance and safety. This is due to an increased number of commercially and militarily applications of UUVs. So far most focus has been directed towards the design of the outer-loop control system, that is speed and positioning control systems while the design of the propeller servo loops have received less attention. An overview of control methods for speed and positioning control of UUVs is found in Fossen [9] and references therein. This paper focuses on the design of a propeller shaft speed controller with feedback from the estimated axial flow velocity u_p in the propeller disc. The motivation for the work is compensation of thruster losses due to variations in the magnitude of the propeller axial flow velocity.

In Yoerger et al. [30] a *one-state model* for propeller shaft speed n with thrust torque T as output is proposed. This model can be written:

$$J_m \dot{n} + K_{n|n|} n |n| = \tau \quad (1)$$

$$T = T(n, u_p) \quad (2)$$

where τ is the control input (shaft torque). It is convenient to assume that $u_p = 0$ when computing T . However, u_p can be measured by using a laser-Doppler velocimeter (LDV) system, a particle image velocimeter (PIV) system or an acoustic Doppler velocimeter system for instance. In

Thor I. Fossen is with the Department of Engineering Cybernetics, Norwegian University of Science and Technology, N-7491 Trondheim, Norway. E-mail: tif@itk.ntnu.no.

Mogens Blanke is with the Department of Automatic Control, Aalborg University, Fredrik Bajers Vej 7C, DK-9240 Aalborg, Denmark. E-mail: blanke@control.auc.dk.

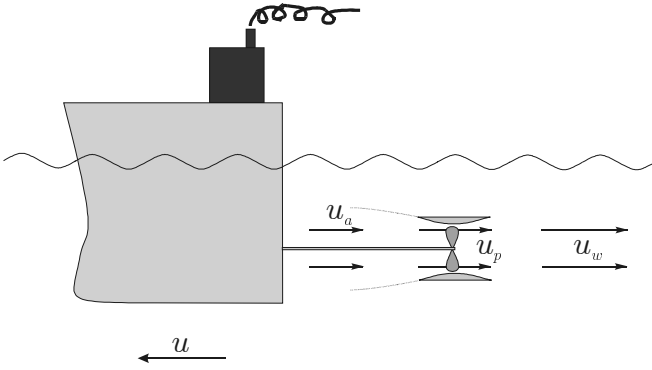


Fig. 1. Definitions of axial flow velocity u_p , advance speed u_a and vehicle speed u .

this article a state observer for reconstruction of u_p will be designed, that is u_p is treated as an unmeasured state.

Healey et al. [12] have modified the models (1)–(2) to describe overshoots in thrust which are typical in experimental data. Based on the results of Cody [6] and McLean [21], Healey and co-workers propose a *two-state model*:

$$J_m \dot{n} + K_n n = \tau - Q \quad (3)$$

$$m_f \dot{u}_p + d_f (u_p - u) |u_p - u| = T \quad (4)$$

$$T = T(n, u_p) \quad (5)$$

$$Q = Q(n, u_p) \quad (6)$$

Here n is the shaft speed, u_p is the axial flow velocity in the propeller disc and u is the forward speed of the vehicle. This was done by modelling a control volume of water around the propeller as a *mass-damper* system. The mass-damper of the control volume interacts with the vehicle speed dynamics which also represents a *mass-damper* system.

Originally Healey et al. [12] considered a *voltage controlled motor*. However, as shown in Appendix A the model representation (3) can be used to describe:

- *Motor (armature) voltage control*
- *Motor (armature) current control*
- *Motor torque control*

The different DC-motor control strategies are obtained by choosing K_n and τ according to Table II in Appendix A. Experimental verifications of the *one-state* and *two-state* models are found in Whitcomb and Yoerger [28].

A more general model is the *three-state* propeller shaft speed model of Blanke, Lindegaard and Fossen [3]:

$$J_m \dot{n} + K_n n = \tau - Q \quad (7)$$

$$m_f \dot{u}_p + d_{f0} u_p + d_f |u_p| (u_p - u_a) = T \quad (8)$$

$$(m - X_{\dot{u}}) \dot{u} - X_u u - X_{u|u} |u| = (1 - t)T \quad (9)$$

$$T = T(n, u_p) \quad (10)$$

$$Q = Q(n, u_p) \quad (11)$$

where damping in surge is modelled as the sum of *linear laminar skin friction*, $-X_u u$, (see Faltinsen and Sortland

[8]) and *nonlinear quadratic drag*, $-X_{u|u} |u| |u|$ (see Faltinsen [7]). Similarly, linear damping, $d_{f0} u_p$, is included in the axial flow model since quadratic damping, $d_f |u_p| u_p$, alone would give an unrealistic response at low speeds (zero quadratic damping at zero speed). However, the linear skin friction gives exponential convergence to zero at low speeds.

The ambient water velocity u_a in (8) is computed by using the steady-state condition:

$$u_a = (1 - w)u \quad (12)$$

where $0 < w < 1$ is the *wake fraction number* (see Lewis [15]).

In the sequel, the unmeasured state u_p will be reconstructed by using a nonlinear state observer. The objective is that propeller thrust $T(n, u_p)$ and torque $Q(n, u_p)$ can be computed for a time-varying u_p , resulting in a more accurate and robust control scheme than conventional shaft speed controllers where this effect is neglected.

A. Propeller Losses

When designing an UUV control system, commanded forces and moments must be realized by a propeller control system using a mapping from thrust demand to propeller revolution. This is a non-trivial task since a propeller in water suffers several phenomena that cause thrust losses. The primaries are:

Axial Water Inflow: Propeller losses caused by axial water inflow, that is the speed u_p of the water going into the propeller. The axial flow velocity will in general differ from the speed of the vehicle. The dynamics of the propeller axial flow is usually neglected when designing the propeller shaft speed controller. This leads to thrust degradation since the computed thruster force is a function of both the propeller shaft speed and axial flow. The magnitude of the axial flow velocity will strongly influence the thrust at high speed so it is crucial for the propeller performance.

Other effects that will reduce the propeller thrust were described in Sørensen et al. [25] and references therein. Some of these effects are:

Cross-Coupling Drag: Water inflow perpendicular to the propeller axis caused by current, vessel speed or jets from other thrusters. This will introduce a force in the direction of the inflow due to deflection of the propeller race.

Air Suction: For heavily loaded propellers ventilation (air suction) caused by decreasing pressure on the propeller blades may occur, especially when the submergence of the propeller becomes small due to the vessel's wave frequency motion.

In-and-out-of Water Effects: For extreme conditions with large vessel motions the *in-and-out-of water effects* will result in a sudden drop of thrust and torque following a hysteresis pattern.

Thruster Hull Interaction: Thrust reduction and change of thrust direction may occur due to thruster-hull interaction caused by frictional losses and pressure effects when

the thruster race sweeps along the hull. The latter is the *Coanda effect* (see Faltinsen [7], pp. 270–272).

Thruster-Thruster Interaction: Thruster-thruster interaction caused by influence from the propeller race from one thruster on neighboring thrusters may lead to significant thrust reduction.

B. Contributions

The main contributions of the paper are a *global exponential stable* (GES) nonlinear observer for estimation of axial flow velocity using vessel speed and propeller revolution measurements (Theorem 1). In addition a nonlinear output feedback propeller shaft speed controller using feedback from the estimate of the axial flow velocity (Theorem 2) is proven to be GES. This is, however, done under the weak assumption that the propeller revolution and axial flow velocity have the same signs. If this assumption is removed, the overall system will be *semi-global exponential stable*.

The nonlinear shaft speed controller compensates for thrust losses due to time variations in axial flow velocity and it is shown to provide superior thrust quality compared to conventional designs. Stability is proven in the framework of Lyapunov stability theory. The proposed output feedback controller is a step towards the design of more sophisticated output feedback shaft speed propeller controllers minimizing some of the propeller losses listed in the previous section.

C. Outline

The paper is outlined as follows: Section II briefly reviews the theory of propeller thrust and torque modelling. Section III describes the modelling of the underwater vehicle dynamics and the axial flow dynamics of the propeller. In Section IV a nonlinear observer for axial flow velocity is proposed while Section V contains a nonlinear output feedback controller for propeller shaft speed using the observer. Section VI extends the results of Section V to integral control. Section VII contains a case study with a UUV driven by a single propeller and Section VIII contains concluding remarks.

II. PROPELLER THRUST AND TORQUE MODELLING

For a fixed pitch propeller the shaft torque Q and force (thrust) T depend on the forward speed u of the vessel, the *advance speed* u_a (ambient water speed) and the propeller rate n , see Figure 1. In addition, other dynamic effects due to *unsteady flows* will influence the propeller thrust and torque. According to Newman [22], Breslin and Andersen [4] and Carlton [5] the following *unsteady flow* effects are significant:

- *air suction*
- *cavitation*
- *in-and-out-of-water effects (Wagner's effect)*
- *wave influenced boundary layer effect*
- *Kuessner effect (gust)*

In this paper we are considering a deeply submerged vessel implying that the first four effects above can be neglected. The *Kuessner effect*, which is caused by a propeller in gust, will appear as a rapid oscillating thrust component. These fluctuations are usually small compared to the total thrust in a dynamical situation. In this paper, we will hence assume that this effect can be neglected as well. We can thus approximate the thrust and torque models with a *quasi-steady* representation. As a result, we limit our discussion to *quasi-steady* thrust and torque modelling while a dynamic model for shaft speed n , advance speed u_a , and surge velocity u will be presented

Unsteady modelling is, however, an important topic for future research since unsteady flow effects are significant in many practical situations in particular for surface vessels. A more detailed discussion on the accuracy of unsteady and quasi-steady modelling is found in Breslin and Andersen [4], pp. 374–386.

A. Quasi-Steady Thrust and Torque

Quasi-steady modelling of thrust and torque are usually done in terms of *lift* and *drag* curves which are transformed to thrust and torque by using the angle of incidence. This approach has been used by Healey et al. [12] and Whitcomb and Yoerger [28] for instance.

The lift and drag are usually represented as *non-dimensional* thrust and torque coefficients computed from self-propulsion tests, see Fossen [9] or Lewis [15]. The *non-dimensional* thrust and torque coefficients K_T and K_Q are computed by measuring T , Q and n . Moreover:

$$K_T(J_0) = \frac{T}{\rho D^4 n |n|}, \quad K_Q(J_0) = \frac{Q}{\rho D^5 n |n|} \quad (13)$$

Here D is the propeller diameter, ρ is the water density and:

$$J_0 = \frac{u_a}{nD} \quad (14)$$

is the *advance ratio*. The numerical expressions for K_T and K_Q are found by *open water* tests, usually performed in a cavitation tunnel or a towing tank. These tests neglect the unsteady flow effects since steady-state values of T , Q and n are used.

The non-dimensional thrust and torque coefficients can also be described by the following parameters (see Oosterveld and van Oossanen [24]):

$$K_T = f_1 \left(J_0, \frac{P}{D}, \frac{A_E}{A_0}, Z \right) \quad (15)$$

$$K_Q = f_2 \left(J_0, \frac{P}{D}, \frac{A_E}{A_0}, Z, R_n, \frac{t}{c} \right) \quad (16)$$

where P/D is the pitch ratio, A_E/A_0 is the expanded-area ratio, Z is the number of blades, R_n is the *Reynolds number*, t is the maximum thickness of the blade section, and c is the chord length of the blade section.

From (13) the thrust T and torque Q can be written

$$T = \rho D^4 K_T(J_0) n |n| \quad (17)$$

$$Q = \rho D^5 K_Q(J_0) n |n| \quad (18)$$

The open water propeller efficiency in undisturbed water is given as the ratio of the work done by the propeller in producing a thrust force divided by the work required to overcome the shaft torque according to:

$$\eta_o = \frac{u_p T}{2\pi n Q} = \frac{J_0}{2\pi} \cdot \frac{K_T}{K_Q} \quad (19)$$

K_T , K_Q , and η_o curves for different pitch ratios for a *Wageningen B-screw series* based on Table 5 in Oosterveld and van Oossanen [24], with $R_n = 2 \cdot 10^6$, $Z = 4$, $D = 3.1$ m, and $A_E/A_o = 0.52$ are shown in Figure 2.

For simplicity we will consider an underwater vehicle where K_T and K_Q show a linear behavior in J_0 . Hence, we suggest to approximate:

$$K_T = \alpha_1 J_0 + \alpha_2 \quad (20)$$

$$K_Q = \beta_1 J_0 + \beta_2 \quad (21)$$

where α_i and β_i ($i = 1, 2$) are four non-dimensional constants. It should be noted that nonlinear functions for K_T and K_Q can also be used. This is equivalent to the *lint theory* result (see Blanke [1]). Formulas (20)–(21) imply that the mathematical expressions for Q and T can be written as (see Fossen [9], pp. 94–97):

$$T = T_{n|n}|n|n| - T_{|n|u_a}|n|u_a \quad (22)$$

$$Q = Q_{n|n}|n|n| - Q_{|n|u_a}|n|u_a \quad (23)$$

where

$$\begin{aligned} Q_{n|n} &= \rho D^5 \beta_2 & T_{n|n} &= \rho D^4 \alpha_2 \\ Q_{|n|u_a} &= \rho D^4 \beta_1 & T_{|n|u_a} &= \rho D^3 \alpha_1 \end{aligned} \quad (24)$$

are *positive* propeller coefficients given by the propeller characteristics. Notice that T and Q are defined for all n even though J_0 is undefined for $n = 0$. This is important since the observer-controller will be based on the expressions for T and Q .

The coefficient $T_{|n|u_a}$ is derived from steady state where u_a has achieved its final value. To explicitly account for the *dynamic variation* in axial water speed, the thrust (22) is modified according to (Blanke et al. [3]):

$$\begin{aligned} T &= T_{n|n}|n|n| - T_{|n|u_a}^o |n|u_a - T_{|n|u_a}^o |n|(u_p - u_a) \\ &= T_{n|n}|n|n| - T_{|n|u_a}^o |n|u_p \end{aligned} \quad (25)$$

where $T_{|n|u_a}^o$ is defined in terms of the steady-state ratio \bar{u}_a/\bar{u}_p , that is:

$$T_{|n|u_a}^o := \frac{\bar{u}_a}{\bar{u}_p} T_{n|n}|n|n| = \frac{1}{1+a} T_{n|n}|n|n| > 0 \quad (26)$$

Here $a > 0$ is an axial flow parameter (see Lewis [15], page 131–132). Similarly, the torque mapping (23) is modified to:

$$Q = Q_{n|n}|n|n| - Q_{|n|u_a}^o |n|u_p \quad (27)$$

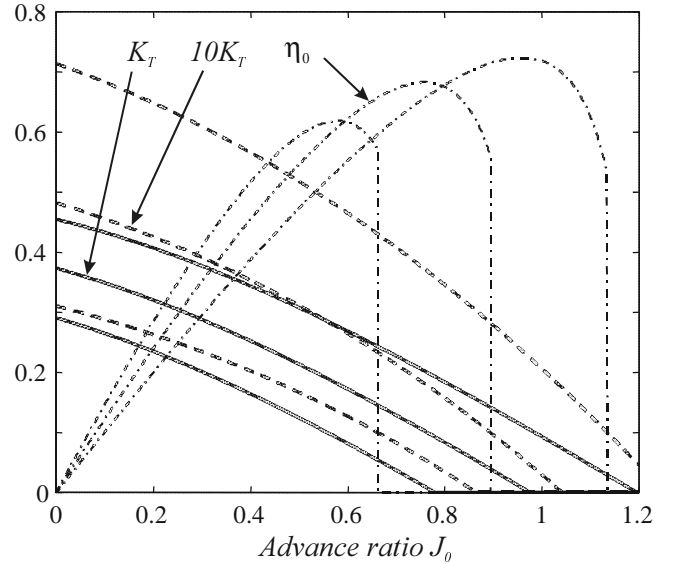


Fig. 2. Open water K_T (solid), $10 \cdot K_Q$ (dash) and η_o (dash-dot) as a function of advance ratio J_0 for $P/D = 0.7, 0.89$ and 1.1 . Reconstructed from data in [24].

III. UUV AND PROPELLER AXIAL FLOW DYNAMICS

Without loss of generality, we will consider an UUV moving in surge (x -direction) equipped with one single propeller aft of the hull. It is also assumed that the propeller is driven by a DC-motor, see Appendix A.

Let u (positive forwards) denote the forward speed of the underwater vehicle. The surge dynamics is assumed coupled to the *axial flow velocity* u_p of the propeller (positive backwards) according to:

$$(m - X_{\dot{u}})\dot{u} - X_u u - X_{u|u}|u|u| = (1 - t)T \quad (28)$$

$$m_f \dot{u}_p + d_{f0} u_p + d_f |u_p| (u_p - u_a) = T \quad (29)$$

where $m_f > 0$, $d_{f0} > 0$ and $d_f > 0$ (see Blanke et al. [3]).

The vessel dynamics in surge (28) is modelled according to Fossen [9] where $m - X_{\dot{u}} > 0$ is the mass of the vessel including hydrodynamic added mass, $-X_u u - X_{u|u}|u|u| \geq 0$ is damping due to *linear skin friction* (see Faltinsen and Sortland [8]) and *quadratic drag* (see Lewis [15]), and $t > 0$ is the thrust deduction number (typically 0.05 – 0.2) due to propeller-hull interactions. Notice that linear damping, $-X_u u$, is added in addition to the quadratic term, $-X_{u|u}|u|u|$. This ensures that u converges exponentially to zero for $T = 0$.

The dynamics of the water (29) due to a control volume surrounding the inlet flow of the propeller is based on the work of Blanke et al. [3] using the ideas of Healey et al. [12], Cody [6] and McLean [21]. Notice that (29) represents a nonlinear “hydrodynamic” mass-damper for $u = 0$.

For a vessel moving at positive cruise-speed in steady flow, $u = \text{constant}$ and $u_a = \text{constant}$. The relationship between ambient water velocity and vehicle speed in steady-state is (see Lewis [15]):

$$u_a = (1 - w)u \quad (30)$$

where $w > 0$ (typically 0.1 – 0.4) is denoted as the *wake fraction number*, see also Sørensen et al. [25].

A. Determination of the UUV Model Parameters

The UUV model parameters can be found by using system identification (SI) methods, see Zhou and Blanke [31] for instance, hydrodynamic computation programs, semi-empirical methods or engineering judgement. For a slender body a first guess could be (see Fossen [9]):

$$-X_{\dot{u}} = (0.05 - 0.10) \cdot m \quad (31)$$

The damping coefficients can be found as:

$$-X_u = \frac{m - X_{\dot{u}}}{T_{\text{surge}}}, \quad -X_{u|u} = \frac{1}{2} \rho C_d A_{\text{surge}} \quad (32)$$

where $T_{\text{surge}} > 0$ is a design parameter (time constant in surge), C_d is the drag coefficient and A_{surge} is the cross-sectional area in surge as defined by *Morrison's equation* (see Lewis [15]). Alternatively, $-X_u$ and $-X_{u|u}$ can be found by performing a *free decay test* (see Faltinsen [7]).

B. Determination of the Axial Flow Parameters

The mass $m_f > 0$ and quadratic damping coefficient $d_f > 0$ of the control volume can be treated as design parameters. A guideline could be to choose (see Healey et al. [12] and Blanke et al. [3]):

$$m_f = \gamma \rho A_p l, \quad d_f = 2 \rho A_p \quad (33)$$

where ρ is the density of water, A_p is the cross-sectional area of the thruster, l is the length of the duct and $\gamma \geq 1.0$ is an empirically determined added mass coefficient. For conventional vehicles $0 < m_f < m$.

Furthermore the thrust deduction and wake fraction numbers are chosen as:

$$\begin{aligned} 0 < t < 1, & \quad (\text{typically } 0.05 - 0.2) \\ 0 < w < 1 & \quad (\text{typically } 0.1 - 0.4) \end{aligned}$$

while the linear damping coefficient $d_{f0} > 0$ is treated as a design parameter:

$$d_{f0} = \frac{m_f}{T_f} \quad (34)$$

where $T_f > 0$ is the time constant corresponding to the linear part of the axial flow dynamics.

C. Resulting Model for Vehicle Speed and Propeller Axial Flow Dynamics

When designing the nonlinear observer the following assumption for the nonlinear term $|u_p|$ is needed:

Assumption A1: Under normal operation of the vehicle it is assumed that axial flow velocity u_p and propeller revolution n have the same signs. This implies that $|u_p| = \text{sign}(u_p)u_p = \text{sign}(n)u_p$.

Under Assumption A1, (25) and (28)–(30) can be combined to give:

$$\begin{aligned} & \begin{bmatrix} m - X_{\dot{u}} & 0 \\ 0 & m_f \end{bmatrix} \begin{bmatrix} \dot{u} \\ \dot{u}_p \end{bmatrix} \\ & + \begin{bmatrix} -X_u - X_{u|u}|u| & \\ & 0 \end{bmatrix} \\ & \begin{bmatrix} 0 \\ d_{f0} + d_f|u_p| - d_f(1-w)\text{sign}(n)u \end{bmatrix} \begin{bmatrix} u \\ u_p \end{bmatrix} \end{aligned} \quad (35)$$

$$\begin{aligned} & + |n| \begin{bmatrix} 0 & (1-t)T_{|n|u_a}^o \\ 0 & T_{|n|u_a}^o \end{bmatrix} \begin{bmatrix} u \\ u_p \end{bmatrix} \\ & = \begin{bmatrix} (1-t)T_{|n|n}|n| \\ T_{|n|n}|n| \end{bmatrix} \end{aligned} \quad (36)$$

The measurement equation is:

$$y = \begin{bmatrix} 1 & 0 \end{bmatrix} \begin{bmatrix} u \\ u_p \end{bmatrix} \quad (37)$$

This can be written in state-space form according to:

$$H\dot{x} + D_0x + D_1(x, n, y)x + |n|Ex = f(n) \quad (38)$$

$$y = h^T x \quad (39)$$

where $x = [u, u_p]^T$, $y = u$ and:

$$\begin{aligned} H &= \begin{bmatrix} m - X_{\dot{u}} & 0 \\ 0 & m_f \end{bmatrix} \\ D_0 &= \begin{bmatrix} -X_u & 0 \\ 0 & d_{f0} \end{bmatrix} \\ D_1(x, n, y) &= \begin{bmatrix} -X_{u|u}|u| & 0 \\ 0 & d_f|u_p| - d_f(1-w)\text{sign}(n)y \end{bmatrix} \\ E &= \begin{bmatrix} 0 & (1-t)T_{|n|u_a}^o \\ 0 & T_{|n|u_a}^o \end{bmatrix} \\ f(n) &= \begin{bmatrix} (1-t)T_{|n|n}|n| \\ T_{|n|n}|n| \end{bmatrix} \\ h^T &= \begin{bmatrix} 1 & 0 \end{bmatrix} \end{aligned}$$

IV. NONLINEAR OBSERVER FOR ESTIMATION OF PROPELLER AXIAL VELOCITY

A nonlinear observer for shaft speed estimation and fault detection has been proposed by Blanke, Izadi-Zamanabadi and Lootsma [2] under the assumption that the effect of the propeller axial inlet flow u_p can be neglected. They have proven semi-global asymptotic and (local) exponential stability for the case with quadratic damping.

Nonlinear observers for underwater vehicles can also be designed by using contraction analysis as described by Lohmiller [17], pp. 38–42, Lohmiller and Slotine [18], [19]. This can be related to the work of Lewis [16] where it is shown that the *Riemann* metric can be used as a tool for contraction analysis of non-autonomous nonlinear systems. Furthermore, combination properties of contracting systems can be exploited to design globally convergent

observer-controllers for shaft speed output feedback control which is attractive due to design simplicity and good convergence properties.

The focus of this paper is Lyapunov-based output feedback control and global exponential stability properties which are important from a robust performance point of view. This gives a different observer structure than the one obtained from contraction analysis. For a more detailed discussion on nonlinear observer-controller design, see Nijmeijer and Fossen [23] and references therein.

A. Observer Equations

In this section, we will derive a nonlinear state observer for the unmeasured state u_p and use this result as a basis for the nonlinear controller. The main motivation for this is that the control law should exploit u_p in the design in order to reduce propeller losses. This is done by choosing the following observer structure copying the dynamics (38)–(39):

$$H\dot{\hat{x}} + D_0\hat{x} + D_1(\hat{x}, n, y)\hat{x} + |n|E\hat{x} = f(n) + k(n)\tilde{y} \quad (40)$$

with output:

$$\hat{y} = h^T\hat{x} \quad (41)$$

where $\tilde{y} = y - \hat{y}$ and an intelligent guess for the observer gain vector is:

$$k(n) = \begin{bmatrix} K_{10} \\ K_{20} \end{bmatrix} + |n| \begin{bmatrix} K_{11} \\ K_{21} \end{bmatrix} \quad (42)$$

The error dynamics corresponding to $\tilde{x} = x - \hat{x}$ becomes:

$$H\dot{\tilde{x}} = -(D_0 + |n|E + k(n)h^T)\tilde{x} - \delta \quad (43)$$

where the nonlinear estimation error term δ is:

$$\begin{aligned} \delta &= D_1(x, n, y)x - D_1(\hat{x}, n, y)\hat{x} \\ &= \begin{bmatrix} (-X_{u|u})|u|u - (-X_{u|u})|\hat{u}|\hat{u} \\ d_f|u_p|u_p - d_f|\hat{u}_p|\hat{u}_p \end{bmatrix} \end{aligned} \quad (44)$$

Defining:

$$F = \begin{bmatrix} -X_u + K_{10} & 0 \\ K_{20} & d_{f0} \end{bmatrix}, \quad G = \begin{bmatrix} K_{11} & (1-t)T_{|n|u_a}^o \\ K_{21} & T_{|n|u_a}^o \end{bmatrix} \quad (45)$$

implies that (43) can be written:

$$H\dot{\tilde{x}} = -F\tilde{x} - |n|G\tilde{x} - \delta \quad (46)$$

We will now show how the elements in the observer gain vector $k(n)$ can be chosen such that the equilibrium point $\tilde{x} = 0$ is GES.

B. Lyapunov Analysis

Consider the Lyapunov function candidate:

$$V_{\text{obs}}(\tilde{x}, t) = \tilde{x}^T H\tilde{x} \quad (47)$$

$$\begin{aligned} \dot{V}_{\text{obs}}(\tilde{x}, t) &= -\tilde{x}^T (F + F^T)\tilde{x} - |n|\tilde{x}^T (G + G^T)\tilde{x} \\ &\quad - 2\tilde{x}^T\delta \end{aligned} \quad (48)$$

where the design goal is to choose K_{10}, K_{20}, K_{11} and K_{21} such that $\dot{V}_{\text{obs}} < 0$ for all $\tilde{x} \neq 0$.

For a *nondecreasing function* $f(x)$ it can be shown that:

$$(x - \hat{x})(f(x) - f(\hat{x})) \geq 0 \quad (49)$$

From (49) it is seen that the nonlinear coupling term $\tilde{x}^T\delta = \tilde{x}_1\delta_1 + \tilde{x}_2\delta_2$ in \dot{V}_{obs} satisfies:

$$\begin{aligned} \tilde{x}^T\delta &= (u - \hat{u})\delta_1 + (u_p - \hat{u}_p)\delta_2 \\ &= (u - \hat{u})(-X_{u|u})(|u|u - |\hat{u}|\hat{u}) \\ &\quad + (u_p - \hat{u}_p)d_f(|u_p|u_p - |\hat{u}_p|\hat{u}_p) \\ &\geq 0 \end{aligned} \quad (50)$$

since $-X_{u|u} > 0$ and $d_f > 0$. This is due to the fact that dissipative damping terms like quadratic drag, $u|u|$, and also higher order terms in $u|u|^n$ ($n = 1, 2, 3, \dots$) are all *nondecreasing*. Therefore:

$$\dot{V}_{\text{obs}}(\tilde{x}, t) \leq -\tilde{x}^T (F + F^T)\tilde{x} - |n|\tilde{x}^T (G + G^T)\tilde{x} \quad (51)$$

Next we notice that the last term in (51) is zero if $n = 0$. For non-zero values of n we therefore require that:

$$G + G^T = \begin{bmatrix} 2K_{11} & (1-t)T_{|n|u_a}^o + K_{21} \\ (1-t)T_{|n|u_a}^o + K_{21} & 2T_{|n|u_a}^o \end{bmatrix} > 0 \quad (52)$$

which is easy to satisfy since K_{11} and K_{21} can be chosen such that:

$$K_{11} > 0 \quad (53)$$

$$4K_{11}T_{|n|u_a}^o > \left((1-t)T_{|n|u_a}^o + K_{21} \right)^2 \quad (54)$$

Hence,

$$\dot{V}_{\text{obs}}(\tilde{x}, t) \leq -\tilde{x}^T (F + F^T)\tilde{x} \quad (55)$$

We will now show that the remaining two gains K_{10} and K_{20} can be chosen such that:

$$\begin{aligned} \dot{V}_{\text{obs}}(\tilde{x}, t) &\leq -\tilde{x}^T (F + F^T)\tilde{x} \\ &\leq -q_1\tilde{u}^2 - q_2\tilde{u}_p^2 \\ &< 0, \forall \tilde{u} \neq 0, \tilde{u}_p \neq 0 \end{aligned} \quad (56)$$

where $q_1 > 0$ and $q_2 > 0$. In order to prove this we will make use of the following lemma:

Lemma 1 (Negative Quadratic Form) The quadratic form:

$$\dot{V} = -x^T P x \quad (57)$$

with $P = \{p_{ij}\}$ is bounded by

$$\dot{V} \leq -q_1 x_1^2 - q_2 x_2^2 \quad (58)$$

where

$$q_1 = p_{11} - \beta > 0 \quad (59)$$

$$q_2 = p_{22} - \frac{(p_{12} + p_{21})^2}{4\beta} > 0, \quad \beta > 0 \quad (60)$$

if:

$$p_{11} > \beta > 0 \quad (61)$$

$$p_{22} > \frac{(p_{12} + p_{21})^2}{4\beta} > 0 \quad (62)$$

Proof: Expanding \dot{V} , yields:

$$\begin{aligned} \dot{V} &= -p_{11}x_1^2 - (p_{12} + p_{21})x_1x_2 - p_{22}x_2^2 \\ &= -(p_{11} - \beta)x_1^2 - \left(\sqrt{\beta}x_1 + \frac{(p_{12} + p_{21})}{2\sqrt{\beta}}x_2 \right)^2 \\ &\quad - \left(p_{22} - \frac{(p_{12} + p_{21})^2}{4\beta} \right) x_2^2 \\ &\leq -\underbrace{(p_{11} - \beta)}_{q_1} x_1^2 - \underbrace{\left(p_{22} - \frac{(p_{12} + p_{21})^2}{4\beta} \right)}_{q_2} x_2^2 \end{aligned} \quad (63)$$

From this it is seen that (61)–(62) implies that $q_1 > 0$ and $q_2 > 0$ and therefore that $\dot{V} < 0$ for all $x_1 \neq 0$ and $x_2 \neq 0$. ■

Theorem 1 (GES Nonlinear Observer Error Dynamics)

The equilibrium point $\tilde{x} = 0$ of the observer error dynamics (46) is GES if K_{11} and K_{21} are chosen such that $G + G^T > 0$, that is:

$$K_{11} > 0 \quad (64)$$

$$4K_{11}T_{|n|u_a}^o > \left((1-t)T_{|n|u_a}^o + K_{21} \right)^2 \quad (65)$$

while K_{10} and K_{20} must satisfy:

$$2d_0\beta > K_{20}^2 \quad (66)$$

$$K_{10} - X_u > \frac{1}{2}\beta \quad (67)$$

where $\beta > 0$.

Proof: Let

$$P = F + F^T = \begin{bmatrix} 2(-X_u + K_{10}) & K_{20} \\ K_{20} & 2d_{f0} \end{bmatrix} \quad (68)$$

in Lemma 1. Hence, $q_1 > 0$ and $q_2 > 0$ require:

$$p_{11} = 2(-X_u + K_{10}) > \beta > 0 \quad (69)$$

$$p_{22} = 2d_{f0} > \frac{K_{20}^2}{\beta} > 0 \quad (70)$$

directly implies (66)–(67). It then follows that $\dot{V} \leq -q_1x_1^2 - q_2x_2^2$ with $q_1 > 0$ and $q_2 > 0$. Hence, it follows from Lyapunov stability theory that the equilibrium point $\tilde{x} = 0$ is GES if $\beta > 0$. ■

Remark 1: It should be noted that GES is proven under Assumption A1, that is $|u_p| = \text{sign}(u_p)u_p \approx \text{sign}(n)u_p$. If this assumption is relaxed by using the estimate $|\hat{u}_p|u$ instead of $\text{sign}(n)\hat{u}_pu$ for the nonlinear coupling term $|u_p|u$, Lyapunov stability analysis can still be used to prove semi-global exponential stability.

Remark 2: It should also be noted that we have not considered bias state estimation when designing the observer. In a practical implementation it might be necessary to augment a constant bias term to the dynamic model in order to improve robustness to unmodelled dynamics and parametric uncertainties. Bias state estimation for ships have been discussed by Fossen and Strand [10] and, Zhou and Blanke [31]

V. DEFINITION OF THE CONTROL PROBLEM

The control objective is to design a propeller shaft speed controller tracking the desired propeller revolution n_d (inner loop controller) by compensating the axial flow velocity u_p . The desired propeller rate of revolution is generated by the UUV speed controller where u_d denotes the desired vessel speed (outer loop controller).

The dynamics of the two control loops can be summarized according to:

A. UUV Speed Control Loop

The surge dynamics of the UUV is:

$$\dot{x} = u \quad (71)$$

$$(m - X_{\dot{u}})\dot{u} - X_u u - X_{u|u}|u| = (1-t)T \quad (72)$$

where T is the control input (force) generated by a speed controller

$$T = T(\dot{u}_d, u_d, u) \quad (73)$$

designed such that $u \rightarrow u_d$.

B. Propeller Shaft Speed Control Loop

The desired shaft speed is found from (25) as:

$$\begin{aligned} n'_d &= \frac{T_{|n|u_a}^o u_p + \text{sign}(T_d) \sqrt{\left((T_{|n|u_a}^o u_p)^2 + 4T_{|n|n}T_d \right)}}{2T_{|n|n}} \\ &= \omega(T_d, u_p) \end{aligned} \quad (74)$$

$$\ddot{n}_d + 2\omega_f \dot{n}_d + \omega_f^2 n_d = \omega_f^2 n'_d, \quad \omega_f > 0 \quad (75)$$

where T_d is the desired thrust and (75) is a 2nd-order low-pass filter with natural frequency ω_f used to generate two smooth reference signal n_d and \dot{n}_d . These signals are again used as reference for the propeller controller:

$$\tau = \tau(\dot{n}_d, n_d, n, u_p) \quad (76)$$

corresponding to the *two-state* actuator dynamics:

$$\dot{n} = \phi_1(n, Q(n, u_p), \tau) \quad (77)$$

$$\dot{V}_a = \phi_2(n, u_p, u) \quad (78)$$

$$T = T(n, u_p) \quad (79)$$

The two control loops are shown in Figure 3 indicating how a nonlinear shaft speed propeller controller together with a conventional UUV speed controller should exploit

the estimate of the propeller axial flow velocity \hat{u}_p . It is also seen that this is a nonlinear output feedback control problem. One solution to this control problem is to apply *observer backstepping* (see Krstic et al. [14]). This is the topic for the next section.

Experiments with different shaft speed control strategies and position control of underwater vehicles are reported in Tsukamoto et al. [26] and Whitcomb and Yoerger [29].

VI. NONLINEAR OUTPUT FEEDBACK CONTROL DESIGN

In this section we will design a nonlinear output feedback propeller controller using only surge speed measurements u and propeller revolution measurements n . The axial flow velocity u_p will be estimated by the state estimator (40)–(41) which was proven to be GES under Assumption A1 (Theorem 1). The design goal is to render the closed-loop error dynamics of the observer-controller GES.

A. Nonlinear Model for Propeller Shaft Speed Control

Consider the unified DC-motor model (Appendix A):

$$J_m \dot{n} + K_n n = \tau - Q(n, u_p) \quad (80)$$

which can be used to describe motor *voltage*, *current* and *torque* controlled propellers. Substituting the expression for Q given by (27) into (80), yields the 3rd-order model:

$$J_m \dot{n} = -(K_n + Q_{n|n|} |n|)n + Q_{|n|u_a}^o |n| u_p + \tau \quad (81)$$

$$H \dot{x} + D_0 x + D_1(x, n, y)x + |n| E x = f(n) \quad (82)$$

$$y = h^T x \quad (83)$$

B. Lyapunov Analysis

The observer (40) is used to generate an estimate \hat{u}_p of u_p . Consider the control Lyapunov function candidate:

$$V = V_{\text{obs}} + \frac{1}{2} J_m \tilde{n}^2 \quad (84)$$

$$\dot{V} \leq -q_1 \tilde{u}^2 - q_2 \tilde{u}_p^2 + J_m \tilde{n} \dot{\tilde{n}} \quad (85)$$

where $\tilde{n} = n - n_d$ is the tracking error. Substituting (81) into (85), yields:

$$\begin{aligned} \dot{V} \leq & -q_1 \tilde{u}^2 - q_2 \tilde{u}_p^2 + \tilde{n} [\tau - J_m \dot{n}_d \\ & - (K_n + Q_{n|n|} |n|)n + Q_{|n|u_a}^o |n| u_p] \end{aligned} \quad (86)$$

The expression for \dot{V} suggests that the control law τ should be chosen to include three parts: (1) a nonlinear P-controller, $-(K_{p0} + K_{p1} n^2) \tilde{n}$, (2) a nonlinear feedforward term based on the measured propeller revolution n and the desired propeller revolution n_d , and (3) a nonlinear cross-term, $-Q_{|n|u_a}^o |n| \hat{u}_p$, compensating for the axial flow into the propeller. This is the main result of the paper.

Theorem 2 (GES Observer-Controller Error Dynamics) Consider the nonlinear shaft speed controller:

$$\begin{aligned} \tau = & \underbrace{-(K_{p0} + K_{p1} n^2) \tilde{n}}_{\text{P-control}} + \underbrace{J_m \dot{n}_d + (K_n + Q_{n|n|} |n|) n_d}_{\text{Reference Feed Forward}} \\ & - \underbrace{Q_{|n|u_a}^o |n| \hat{u}_p}_{\text{Axial Flow Compensator}} \end{aligned} \quad (87)$$

with

$$K_{p0} > 0, \quad K_{p1} > \frac{1}{4} (Q_{|n|u_a}^o)^2 > 0 \quad (88)$$

Let the estimate \hat{u}_p be generated by using the nonlinear observer (40)–(41) with $q_2 > 1$ in Lemma 1 implying that K_{20} must satisfy $2d_{f0} > 1 + K_{20}^2/\beta$. Hence, the equilibrium point $(\tilde{u}, \tilde{u}_p, \tilde{n}) = (0, 0, 0)$ of the observer-controller error dynamics:

$$M \dot{\tilde{v}} + D(\nu) \tilde{v} + d = 0 \quad (89)$$

where $v = [u, u_p, n]^T$ and:

$$\begin{aligned} M &= \begin{bmatrix} m - X_{\dot{u}} & 0 & 0 \\ 0 & m_f & 0 \\ 0 & 0 & J_m \end{bmatrix} \\ D(\nu) &= \begin{bmatrix} -K_{10} - K_{11} |n| - X_u & (1-t) T_{|n|u_a}^o |n| \\ -K_{20} - K_{21} |n| & d_{f0} + T_{|n|u_a}^o |n| \\ 0 & -Q_{|n|u_a}^o |n| \\ 0 & \\ 0 & \\ K_{p0} + K_{p1} n^2 + K_n + Q_{n|n|} |n| \end{bmatrix} \\ d &= \begin{bmatrix} (-X_{u|u}) [u |u| - |u - \tilde{u}| (u - \tilde{u})] \\ d_f [|u_p| u_p - |u_p - \tilde{u}_p| (u_p - \tilde{u}_p)] \\ 0 \end{bmatrix} \end{aligned}$$

is GES.

Proof: Substituting (87) into (86), yields:

$$\begin{aligned} \dot{V} \leq & -q_1 \tilde{u}^2 - q_2 \tilde{u}_p^2 + Q_{|n|u_a}^o |n| \tilde{u}_p \tilde{n} \\ & - (K_{p0} + K_{p1} n^2 + K_n + Q_{n|n|} |n|) \tilde{n}^2 \end{aligned} \quad (90)$$

Using the fact that

$$\begin{aligned} - \left(\frac{1}{2} Q_{|n|u_a}^o |n| \tilde{n} - \tilde{u}_p \right)^2 &= -\frac{1}{4} (Q_{|n|u_a}^o)^2 n^2 \tilde{n}^2 \\ &+ Q_{|n|u_a}^o |n| \tilde{n} \tilde{u}_p - \tilde{u}_p^2 \end{aligned}$$

Hence, the cross term in (90) can be replaced by:

$$\begin{aligned} Q_{|n|u_a}^o |n| \tilde{n} \tilde{u}_p &= - \left(\frac{Q_{|n|u_a}^o}{2} |n| \tilde{n} - \tilde{u}_p \right)^2 \\ &+ \frac{(Q_{|n|u_a}^o)^2}{4} n^2 \tilde{n}^2 + \tilde{u}_p^2 \end{aligned} \quad (91)$$

implying that:

$$\begin{aligned} \dot{V} &\leq -q_1 \tilde{u}^2 - (q_2 - 1) \tilde{u}_p^2 - \left(K_{p1} - \frac{1}{4} (Q_{|n|u_a}^o)^2 \right) n^2 \tilde{n}^2 \\ &\quad - \left(\frac{1}{2} Q_{|n|u_a}^o |n| \tilde{n} - \tilde{u}_p \right)^2 \\ &\quad - (K_{p0} + K_n + Q_{n|n}|n|)^2 \tilde{n}^2 \\ &< 0, \forall \tilde{u} \neq 0, \tilde{u}_p \neq 0, \tilde{n} \neq 0 \end{aligned} \quad (92)$$

Hence, according to Lyapunov stability theory the equilibrium point $(\tilde{u}, \tilde{u}_p, \tilde{n}) = (0, 0, 0)$ of the observer-controller error dynamics (89) is GES if $q_1 > 0, q_2 > 1, K_{p0} > 0$ and $K_{p1} > (1/4)(Q_{|n|u_a}^o)^2$. ■

VII. EXTENSIONS TO INTEGRAL CONTROL

When implementing the shaft speed propeller controller, it is important to include integral action in order to compensate for non-zero slowly-varying disturbances and unmodelled dynamics. This can be done by augmenting a constant bias term b to (80) according to:

$$J_m \dot{n} = -K_n n + \tau - Q(n, u_p) + b \quad (93)$$

$$\dot{b} = 0 \quad (94)$$

Choosing the nonlinear control law of PI-type with reference feedforward and axial flow compensation, that is:

$$\begin{aligned} \tau &= \underbrace{-(K_{p0} + K_{p1} n^2) \tilde{n} - \hat{b}}_{\text{PI-control}} \\ &\quad + \underbrace{J_m \dot{n}_d + (K_n + Q_{n|n}|n|) n_d}_{\text{Reference Feed Forward}} \\ &\quad - \underbrace{Q_{|n|u_a}^o |n| \hat{u}_p}_{\text{Axial Flow Compensator}} \end{aligned} \quad (95)$$

$$\dot{b} = K_i \tilde{n}, \quad K_i > 0 \quad (96)$$

implies that (89) takes the form:

$$\dot{x}_1 = h(x_1, t) + g x_2 + d \quad (97)$$

$$\dot{x}_2 = -K_i g^T x_1 \quad (98)$$

with $x_1 = \tilde{v} \in \mathfrak{R}^3, x_2 = \hat{b} - b \in \mathfrak{R}$ and

$$h(x_1, t) = -M^{-1} D(x_1 + \nu_d(t)) x_1 \quad (99)$$

$$g = M^{-1} \begin{bmatrix} 0 \\ 0 \\ -1 \end{bmatrix} = \begin{bmatrix} 0 \\ 0 \\ -1/J_m \end{bmatrix} \quad (100)$$

$$d = -M^{-1} d \quad (101)$$

where we have used that $\nu = x_1 + \nu_d$. The error dynamics (97)–(98) is a *nonlinear non-autonomous* system complicating the Lyapunov stability analysis since $\dot{V} \leq 0$ is only

negative semi-definite. Hence, *LaSalle-Krazovskii's theorem* for invariant manifolds cannot be used (see Khalil [13]) to prove uniformly globally asymptotic stability (UGAS). However, UGAS and uniformly locally exponentially stability (ULES) of the equilibrium point $(x_1^T, x_2) = (0, 0, 0, 0)$ of the error dynamics (97)–(98) can be proven by applying the main result of Loria, Fossen and Teel [20] which is a theorem for "*backstepping with integral action*" (see also Fossen, Loria and Teel [11]). The interested reader is recommended to consult [11] and [20] for the technicalities regarding the proof.

VIII. CASE STUDY

In the simulation study the following two controllers were compared:

- *Nonlinear output feedback integral control* where the nonlinear observer (Theorem 1) was simulated by using the following gains:

$$\begin{aligned} \beta &= -10 X_u \\ K_{10} &= 1.0 \cdot (m - X_{\dot{u}}), \quad K_{20} = 0.1 \cdot m_f \\ K_{11} &= 0.005 \cdot (m - X_{\dot{u}}), \quad K_{21} = -30 \end{aligned}$$

while the control gains in (Theorem 2) were chosen as:

$$K_{p0} = 1.0, \quad K_{p1} = \frac{1}{4} (Q_{|n|u_a}^o)^2, \quad K_i = 1.0$$

When simulating the observer-controller it is noticed that performance improvements can be obtained by reducing the controller gains in particular if the measurements are noisy. It is well known that the gain requirements imposed by the Lyapunov analysis are rather conservative. Moreover, the closed-loop system can be exponential stable for much smaller gains than those given by Theorem 2. In fact, we noticed that the performance was significantly improved when K_{p1} was reduced by a factor of 10 and this did not affect the stability of the closed-loop system.

- *Conventional shaft speed control of PI-type:*

$$\tau = -K_p (n - n_d) - K_i \int_0^t (n - n_d) d\tau \quad (102)$$

with

$$K_p = 10.0, \quad K_i = 1.0$$

For both controllers the torque controlled representation of the DC-motor (118) was used.

A. Model Parameters

The model parameters are given in Table I. The propeller characteristics were taken from an experiment with a full-scale propeller, see Figure 4.

TABLE I
MODEL PARAMETERS.

| | | | |
|----------------|--|-------------|-------------------------------|
| m | $= 1000$ (kg) | D | $= 0.30$ (m) |
| $-X_{\dot{u}}$ | $= 0.05m$ (kg) | ρ | $= 1025$ (kg/m ³) |
| $-X_u$ | $= \frac{m-X_{\dot{u}}}{5.0}$ (kg/s) | w | $= 0.2$ |
| $-X_{u u }$ | $= \frac{\rho C_d A_{surge}}{2}$ (kg/m) | t | $= 0.1$ |
| d_f | $= 2\rho A_p$ (kg/s) | J_m | $= 1.0$ (kgm ²) |
| d_{f0} | $= \frac{m_f}{0.05}$ (kg/m) | C_d | $= 1.0$ |
| m_f | $= \gamma\rho Al$ (kg) | A_{surge} | $= 1.0$ (m ²) |
| l | $= 0.30$ (m) | γ | $= 1.0$ |
| A_p | $= \pi \left(\frac{D}{2}\right)^2$ (m ²) | | |

Least-squares curve fitting of K_T and K_Q gave the following results (straight lines in Figure 4):

$$K_T = -0.9435 J_0 + 0.4243 \quad (103)$$

$$K_Q = -0.1212 J_0 + 0.0626 \quad (104)$$

Even though this over-all linear approximation is crude, in particular for reverse conditions ($J_0 < 0$), the observer is able to cope with the model inaccuracies and give a useful estimate of u_p .

For simulation convenience the values for $T_{|n|u_a}^o$ and $Q_{|n|u_a}^o$ were chosen equal to $T_{|n|u_a}$ and $Q_{|n|u_a}$ which again were computed from the K_T and K_Q mappings.

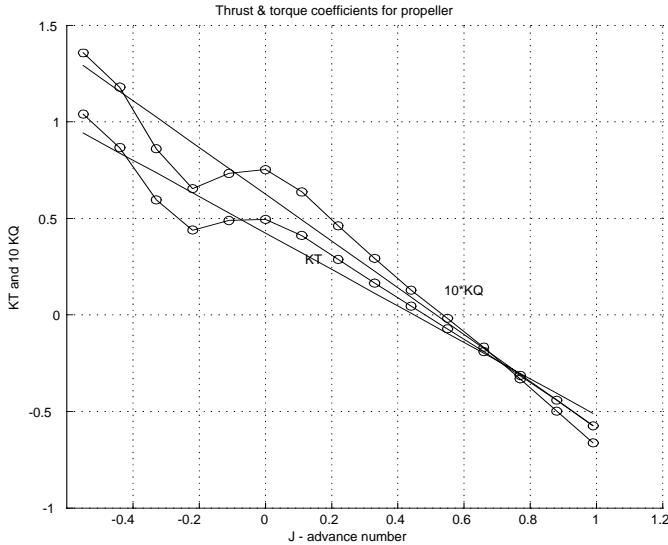


Fig. 3. Experimental results for K_T and $10K_Q$ versus J_0 (circles) and least-squares fits to a straight line (solid lines).

B. Discussion of Simulation Results

The control laws were simulated by commanding a reference thrust of $T_d = 100$ (N) which was shifted to $T_d = -100$ (N) at $t = 30$ (sec), see Figure 6. The results from the simulation study can be summarized according to:

Estimation of Axial Flow Velocity Figure 5 shows the performance of the nonlinear observer. Both estimation errors $\tilde{u}_p = u_p - \hat{u}_p$ and $\tilde{u} = u - \hat{u}$ (upper plots) are zero mean white noise processes. Even though the surge measurement u and shaft speed measurement n are corrupted with white noise with amplitudes 0.1 (m/s) and 0.1 (rps), and standard deviations of $\sigma = 0.0335$ in the simulation study, excellent convergence of $\hat{u}_p \rightarrow u_p$ is obtained (lower left plot). The estimate \hat{u}_p is, however, more noisy than its true value u_p . This can be further improved by tuning of the observer gains. In addition, we see that we obtain good filtering of the noisy signal u (lower right plot).

Thrust Tracking Capabilities From Figure 6 it is seen that the output feedback integral controller has excellent thrust tracking capabilities (lower plots) while an offset in thrust $\tilde{T} = T - T_d$ is observed for the PI-controller (see Figure 7). The desired thrust $T_d = \pm 100$ (N) is transformed to shaft speed reference signals \hat{n}_d and n_d by using (74)–(75). The offset in thrust for the PI-controller is due to variations in axial flow velocity u_p . This is seen by plotting the components:

$$T_0 = T_{|n|n}|n|, \quad Q_0 = Q_{|n|n}|n| \quad (105)$$

$$T_1 = -T_{|n|u_a}^o |n| u_p, \quad Q_1 = -Q_{|n|u_a}^o |n| u_p \quad (106)$$

together with the total thrust $T = T_0 + T_1$ and torque $Q = Q_0 + Q_1$. The PI-controller tracks $T = T_0 = T_d$ (the term T_1 is not available since u_p is unknown when using a PI-controller) while the nonlinear output feedback integral controller uses the estimate \hat{u}_p to track the total thrust $T = T_0 + T_1 = T_d$. Another benefit of using the nonlinear observer in conjunction with an output feedback integral controller is that the estimate \hat{u}_p can be used to compute a more accurate shaft speed reference n_d from T_d . This is seen from (74) where u_p is needed.

RPM Tracking Capabilities and Motor Torque Commands Figures 8 and 9 show the shaft speed tracking performance for the two controllers and the corresponding motor torque commands (control inputs). Since the PI-controller does not use model information a high gain is needed in order to obtain good shaft speed tracking capabilities. This results in more noisy motor torque control signals than for the model-based nonlinear output feedback integral controller. It is also seen that the tracking performance for the nonlinear controller is better than the PI-controller mainly due to compensation of axial flow velocity effects.

IX. CONCLUSIONS

A high performance nonlinear output feedback integral controller for propeller shaft speed was presented in this paper. The control law was designed by first designing a nonlinear observer for the propeller axial flow velocity and next using observer backstepping to produce a globally exponentially stable controller. The control law was also modified to include integral action resulting in a uniformly globally asymptotically and uniformly locally exponentially stable integral controller. The proposed output

feedback controller was shown to be robust for disturbances in propeller revolution and torque.

The case study was an unmanned underwater vehicle propelled with a single main propeller. The propeller was assumed driven by a DC motor and a simulation study was used to demonstrate the tracking capabilities of the observer and controller. The observer was capable of producing accurate estimates of the advance speed. Hence, this estimate could be used to compensate the effect of axial flow velocity on the propeller thrust and torque. The estimate of the axial flow velocity could also be used to compute more accurate set-points for the vehicle speed controller since the thrust commands could be more accurately mapped to propeller revolution commands.

APPENDIX A: DC-MOTOR DYNAMICS

Consider a DC-motor (see Fossen [9]):

$$L_a \frac{d}{dt} i_m = -R_a i_m - K_m \omega_m + V_m \quad (107)$$

$$J_m \dot{n} = K_m i_m - Q \quad (108)$$

where V_m is the armature voltage, i_m is the armature current, n is the propeller revolution and Q is the load from the propeller. In addition, L_a is the armature inductance, R_a is the armature resistance, K_m is the motor torque constant and J_m is the rotor moment of inertia.

Since the electrical time constant $T_a = L_a/R_a$ is small compared to the mechanical time constant, time scale separation suggests:

$$\frac{L_a}{R_a} \frac{d}{dt} i_m \approx 0 \quad (109)$$

Hence, the shaft speed dynamics is given by:

$$0 = -R_a i_m - K_m n + V_m \quad (110)$$

$$J_m \dot{n} = K_m i_m - Q \quad (111)$$

Motor Current Control

The motor current can be controlled by using a P-controller:

$$V_m = K_p(i_d - i_m), \quad K_p > 0 \quad (112)$$

where i_d is the desired motor current. From (110) we get:

$$(R_a + K_p)i_m = -K_m n + K_p i_d \quad (113)$$

The motor dynamics (111) for the current controlled motor therefore takes the form:

$$J_m \dot{n} + \frac{K_m^2}{R_a + K_p} n = \frac{K_m K_p}{R_a + K_p} i_d - Q \quad (114)$$

If a high gain controller $K_p \gg R_a > 0$ is used, this expression simplifies to:

$$J_m \dot{n} = K_m i_d - Q \quad (115)$$

Motor Torque Control

For a DC motor the motor torque will be proportional with the motor current. Hence, the desired motor torque Q_d can be written as:

$$Q_d = K_m i_d \quad (116)$$

From (114) we see that this yields the following dynamics for a torque controlled motor:

$$J_m \dot{n} + \frac{K_m^2}{R_a + K_p} n = \frac{K_p}{R_a + K_p} Q_d - Q \quad (117)$$

which reduces to

$$J_m \dot{n} = Q_d - Q \quad (118)$$

for $K_p \gg R_a > 0$.

Motor Voltage Control

Motor voltage control is obtained by combining (110)–(111) to yield:

$$J_m \dot{n} + \frac{K_m^2}{R_a} n = \frac{K_m}{R_a} V_m - Q \quad (119)$$

Unified DC-Motor Control Model

Based on the three models presented above, a unified control model for the DC-motor shaft speed dynamics can be written:

$$J_m \dot{n} + K_n n = \tau - Q \quad (120)$$

where motor *voltage*, *current* and *torque* control are obtained by choosing the control input τ and linear damping coefficient K_n according to Table II:

TABLE II
DC-MOTOR CONTROL MODEL.

| | control input τ | Linear damping K_n |
|---------|---------------------------------|---------------------------|
| Voltage | $\frac{K_m}{R_a} V_m$ | $\frac{K_m^2}{R_a}$ |
| Current | $\frac{K_m K_p}{R_a + K_p} i_d$ | $\frac{K_m^2}{R_a + K_p}$ |
| Torque | $\frac{K_p}{R_a + K_p} Q_d$ | $\frac{K_m^2}{R_a + K_p}$ |

ACKNOWLEDGMENTS

The authors are grateful to Professors Knut Minsaas and Asgeir J. Sørensen at the Department of Marine Hydrodynamics, the Norwegian University of Science and Technology (NTNU) for useful discussions on steady and unsteady flow effects for propellers. In addition Karl Petter Lindegaard at the Department of Engineering Cybernetics, NTNU should be thanked for his discussions on propeller modelling.

Parts of this work were performed while the first author visited the Department of Automatic Control, Aalborg University, Denmark in the period January-March 1999. The same author is grateful to the Department of Automatic Control, Aalborg University and the Norwegian Research Council for financial support in this period.

BIOGRAPHIES

Thor I. Fossen was born in 1963 in Norway. He received the M.Sc. degree in Naval Architecture in 1987 from the Norwegian University of Science and Technology (NTNU), Trondheim and the Ph.D. degree in Engineering Cybernetics from NTNU in 1991. In the period 1989-1990 Fossen pursued postgraduate studies as a Fulbright scholar in flight control at the Department of Aeronautics and Astronautics, University of Washington, Seattle. In May 1993 Fossen was appointed as a Professor in Guidance, Navigation and Control at the Department of Engineering Cybernetics at NTNU where he is teaching ship and ROV control systems design, flight control, and nonlinear and adaptive control theory.



Fossen is Scientific Advisors for ABB Industri AS, Marine Division and Marintek. In cooperation with ABB he has developed a nonlinear dynamic positioning (DP) system for free-floating and moored ships and a nonlinear and passive state estimator for marine vessels. He has also designed software for identification of ship dynamics from sea-trials. The most outstanding achievement is a weather optimal positioning control for marine vessels minimizing fuel consumption and emission of CO_x/NO_x (Patent NO-19985388). Fossen is the designer of the SeaLaunch trim and heel correction systems. SeaLaunch is a free-floating platform built by Boeing-Energia-Kværner from which the first rocket was launched outside Hawaii in March 1999.

Fossen is the author of the book *Guidance and Control of Ocean Vehicles* (Wiley, 1994) and the co-editor of the book *New Directions in Nonlinear Observer Design* (Springer-Verlag, 1999). Fossen has authored more than 100 scientific articles and book chapters on guidance, navigation and control. Fossen has served as advisor to 11 Ph.D. students and over 80 M.Sc. students. He is a member of IEEE and the Chair of the IEEE Oceanic Engineering/Control Systems Joint Society Chapter of the Norway Section.



Mogens Blanke was born in 1947 in Copenhagen, Denmark. He received the M.Sc. and Ph.D. degrees in automatic control from the Technical University of Denmark (DTU) in 1974 and 1982, respectively. He was a systems analyst at the European Space Agency in the Netherlands in 1975-76, assistant and later associate professor of control engineering at DTU from 1976 to 1985. He was head of the Marine Division of the Automation Company Søren T. Lyngsø A/S from 1985 until 1990 where main activities included total ship integrated control and diesel engine control. He is Professor of Control Systems at Aalborg University since 1990, where he started the research group in autonomous systems and fault-tolerant control. The group's most visible achievement was the autonomous attitude control system for the first Danish satellite, which has been in orbit since early 1999.

Research interests include identification and control of continuous, non-linear systems, estimation and fault detection, and design methods for fault tolerant control. His personal application interests include spacecraft attitude control, automatic steering and rudder-roll damping for ships, and control systems for ship propulsion.

Mogens Blanke is a senior member of IEEE, and he is active in IFAC, the International Federation of Automatic Control. He initiated the IFAC Working Group on Marine Systems in 1986, chaired this and the later technical committee and is presently a member of the IFAC Council.

Mogens Blanke received the Radio Parts Award in 1985, the Esso Price in 1986 and, jointly with the satellite control team in Aalborg, the Aalborg City Springtime Award in 1999.

REFERENCES

- [1] M. Blanke. Ship Propulsion Losses Related to Automated Steering and Prime Mover Control, *The Technical University of Denmark, Lyngby, Ph. D. dissertation*, 1981
- [2] M. Blanke, R. Izadi-Zamanabadi and T. F. Lootsma. Fault Monitoring and Reconfigurable Control for a Ship Propulsion Plant. *Journal of Adaptive Control and Signal Processing, Vol. 12, pp. 671-688, December 1998.*
- [3] M. Blanke, K. P. Lindegaard and T. I. Fossen. Dynamic Model for Thrust Generation of Marine Propellers. *Proceedings of the IFAC Conference of Manoeuvring of Marine Craft (MCMC'2000)*, Aalborg, Denmark, 23-25 August, 2000.
- [4] J. P. Breslin and P. Andersen. *Hydrodynamics of Ship Propellers*. Cambridge University Press, UK, 1994.
- [5] J. S. Carlton. *Marine Propellers and Propulsion*. Oxford: Butterworth-Heinemann, 1994.
- [6] S. E. Cody. An Experimental Study of the Response of Small Thrusters to Step and Triangular Wave Inputs, *MSME thesis, Naval Postgraduate School, Monterey, CA*, 1992.
- [7] O. M. Faltinsen. *Sea Loads and Offshore Structures*. Cambridge University Press, UK, 1990.
- [8] O. M. Faltinsen and B. Sortland. Slow Drift Eddy Making Damping of a Ship. *Applied Ocean Research, AOR-9(1):37-46.*
- [9] T. I. Fossen. *Guidance and Control of Ocean Vehicles*, John Wiley & Sons Ltd., 1994.
- [10] T. I. Fossen and J. P. Strand. Passive Nonlinear Observer Design for Ships Using Lyapunov Methods: Full-Scale Experiments With a Supply Vessel. *Automatica, AUT-35(1)3-16*, 1999.
- [11] T. I. Fossen, A. Loria and A. Teel. A Theorem for UGAS and ULES of Nonautonomous Systems: Robust Control of Mechanical Systems and Ships, *International Journal of Robust and Nonlinear Control*, to appear in 2000.
- [12] A. J. Healey, S. M. Rock, S. Cody, D. Miles and J. P. Brown. Toward an Improved Understanding of Thruster Dynamics for Underwater Vehicles, *IEEE Journal of Oceanic Engineering, JOE-29(4):354-361*, 1995.
- [13] H. Khalil. *Nonlinear Systems*. McMillan Publishing Co., 2nd Edition, New York, 1996.
- [14] M. Krstic, I. Kanellakopoulos and P. Kokotovic. *Nonlinear and Adaptive Control Design*. John Wiley & Sons Ltd.
- [15] E. V. Lewis (Ed.). *Principles of Naval Architecture*, SNAME, 1988.
- [16] P. C. Lewis. Differential Equations Referred to a Variable Metric. *American Journal of Mathematics, AJM-73:48-58*, 1951.
- [17] W. S. Lohmiller. Contraction Analysis of Nonlinear Systems. *Ph.D. Dissertation, Department of Mechanical Engineering, MIT, MA, February 1999.*
- [18] W. Lohmiller and J.-J. Slotine. On Metric Controllers and Observers for Nonlinear Systems. *Proc. of the 35th Conf. on Decision and Control*, Kobe, Japan, pp. 1477-1482, December 1996.
- [19] W. Lohmiller and J.-J. Slotine. On Contraction Analysis for Nonlinear Systems, *Automatica AUT-6*, 1998.
- [20] A. Loria, T. I. Fossen and A. Teel. UGAS and ULES of Non-Autonomous Systems: Applications to Integral Control of Ships and Robot Manipulators, *Proc. of the European Control Conference (ECC'99)*, Karlsruhe, Germany, August 1999.
- [21] M. B. McLean. Dynamic Performance of Small Diameter Tunnel Thrusters, *MSME thesis, Naval Postgraduate School, Monterey, CA*, 1991.
- [22] J. N. Newman *Marine Hydrodynamics*. MIT Press, Cambridge, Massachusetts, 1977.
- [23] H. Nijmeijer and T. I. Fossen (Eds.). *New Directions in Nonlinear Observer Design*. Springer-Verlag London Ltd., 1999.
- [24] M. W. C. Oosterveld and P. van Oossanen. Further Computer-Analyzed Data of the Wageningen B-Screw Series. *Int. Shipbuilding Progress, ISP-22:251-262*, 1975.
- [25] A. J. Sørensen, A. K. Ådnanes, T. I. Fossen and J. P. Strand. A New Method of Thruster Control in Positioning of Ships Based on Power Control, *Proc. of the 4th IFAC Conference on Manoeuvring and Control of Marine Craft, 10-12 September, 1997, Brijuni, Croatia.*
- [26] C. L. Tsukamoto, W. Lee, J. Yuh, K. Choi and J. Lorentz. Comparison Study on Advanced Thruster Control of Underwater Robots. *Proc. of the Int. Conf. on Robotics and Automation*, Albuquerque, New Mexico, pp. 1845-1850, April 1997.
- [27] L. L. Whitcomb and D. R. Yoerger. Comparative Experiments in the Dynamics and Model-Based Control of Marine Thrusters. *Proc. of the IEEE/MTS Oceans'95, Vol. 2, pp. 1019-1028, 1995.*
- [28] L. L. Whitcomb and D. Yoerger. Development, Comparison, and Preliminary Experimental Validation of Nonlinear Dynamic Thruster Models. *IEEE Journal of Oceanic Engineering, JOE-24(4):481-494*, 1999.
- [29] L. L. Whitcomb and D. Yoerger. Preliminary Experiments in Model-Based Thruster Control for Underwater Vehicle Position Control. *IEEE Journal of Oceanic Engineering, JOE-24(4):495-506*, 1999.
- [30] D. R. Yoerger, J. G. Cooke and J.- J. E. Slotine. The Influence of Thruster Dynamics on Underwater Vehicle Behavior and their Incorporation into Control System Design, *IEEE Journal of Oceanic Engineering, JOE-15(3):167-178*, 1991.
- [31] W. W. Zhou and M. Blanke. Identification of a Class of Non-linear State-Space Models Using RPE Techniques. *IEEE Trans. on Automatic Control, TAC-34(3):312-316*, 1989.

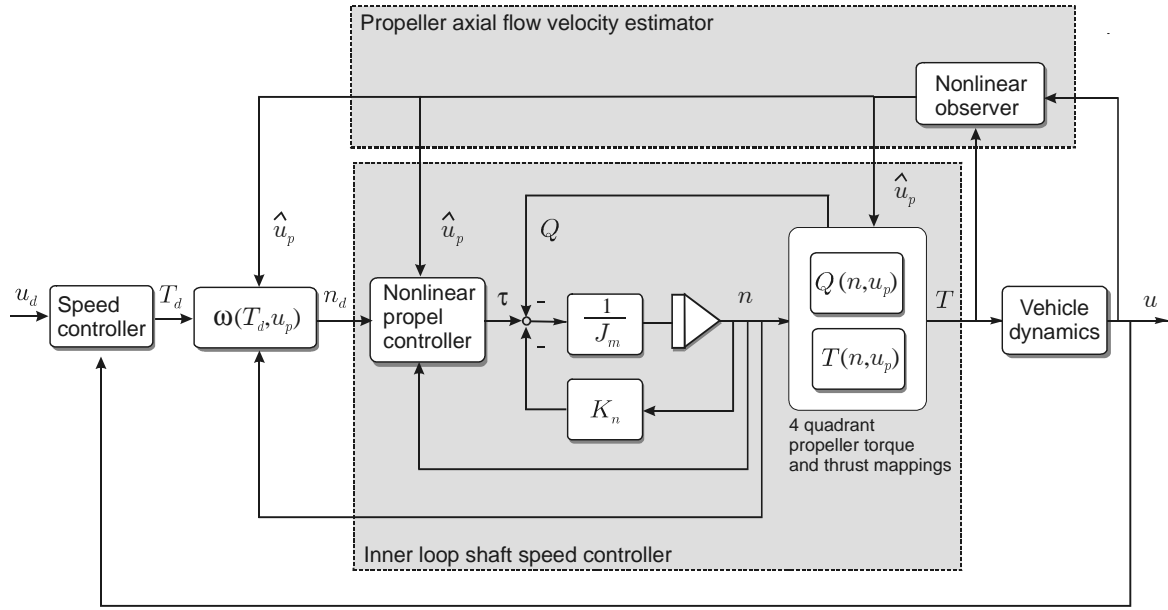


Fig. 4. Block diagram showing the two control loops.

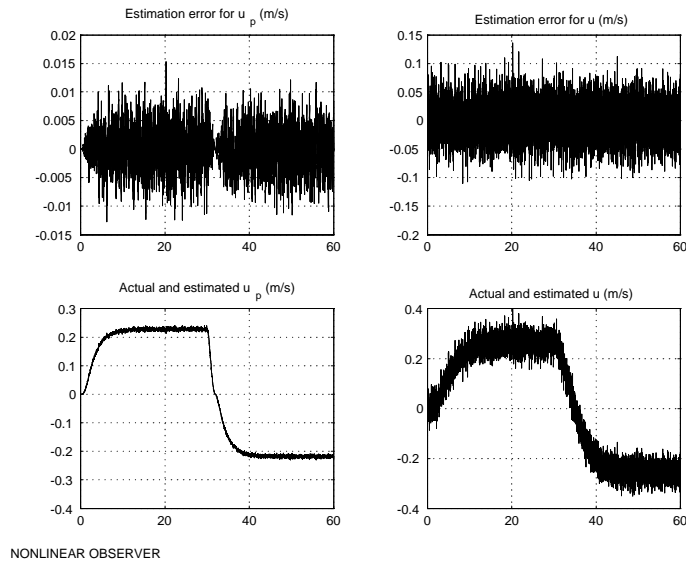


Fig. 5. Upper plots: estimation errors \hat{u}_p and \hat{u} versus time. Lower plots: actual axial flow velocity u_p and measured surge speed u together with their estimates \hat{u}_p and \hat{u} versus time.

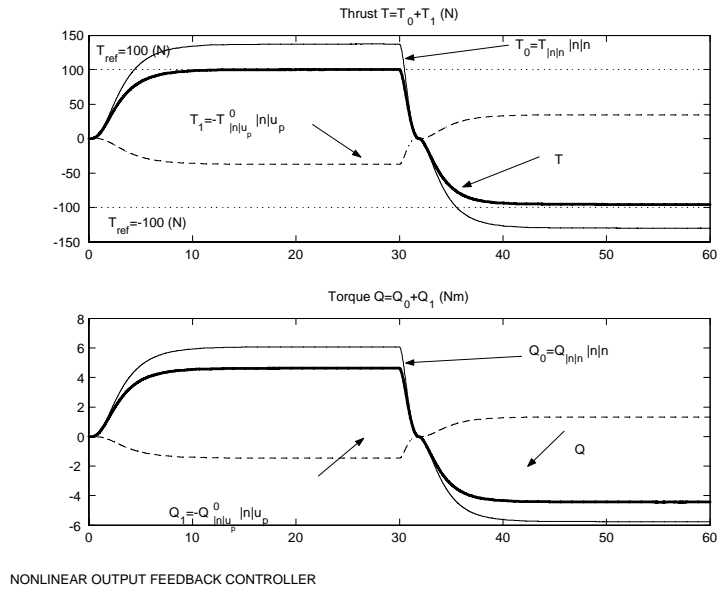


Fig. 6. Thrust T and torque Q for the nonlinear output feedback controller versus time.

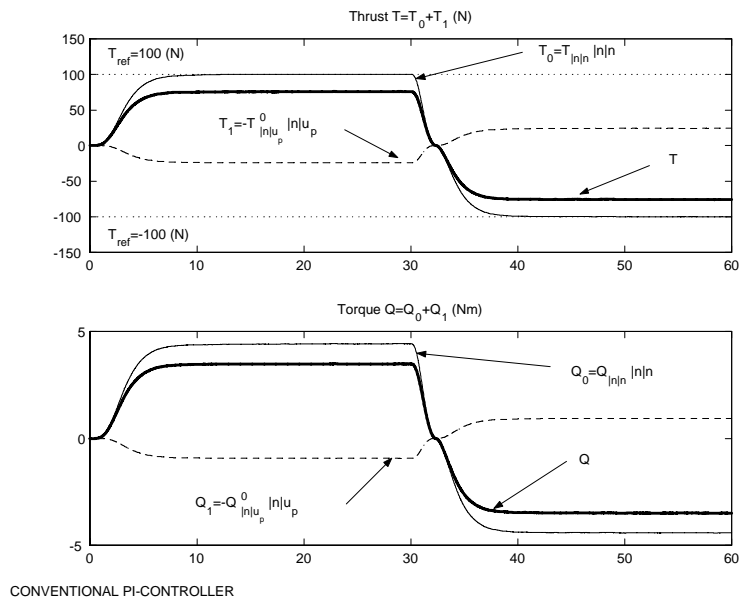


Fig. 7. Thrust T and torque Q for the PI-controller versus time. Notice the steady state offset in thrust.

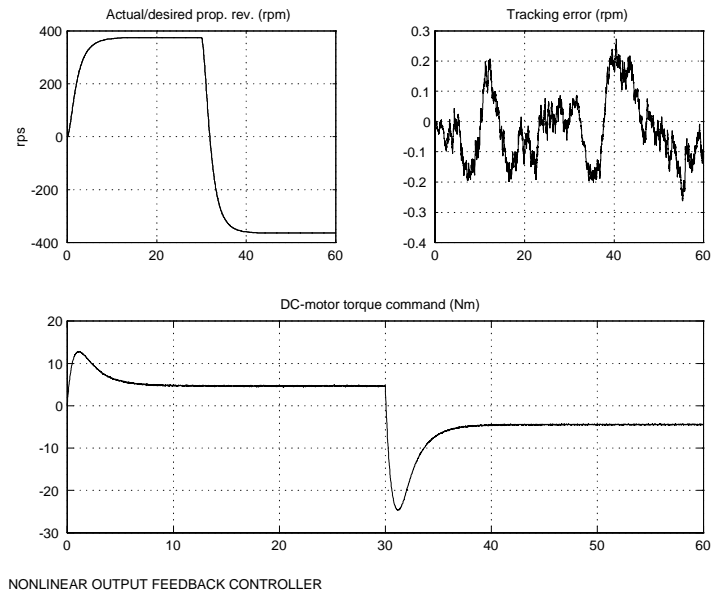


Fig. 8. Actual, n , and desired, n_d , propeller revolutions, tracking errors, $n - n_d$, and motor torque, Q_d , commands the nonlinear output feedback controller versus time.

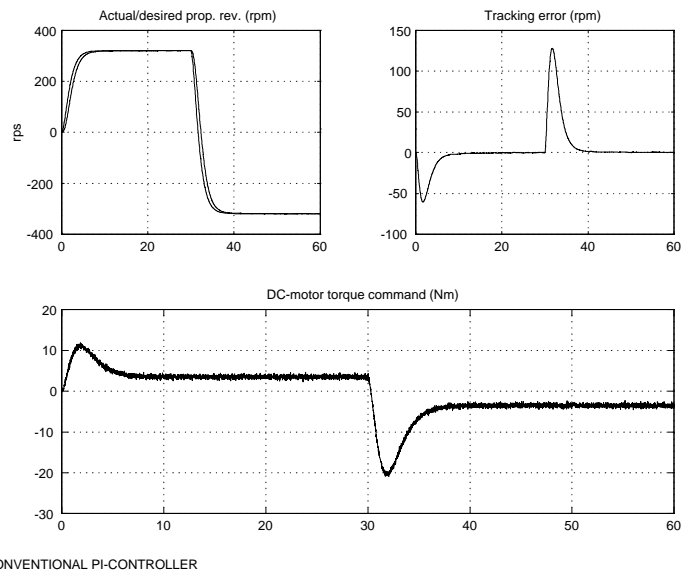


Fig. 9. Actual, n , and desired, n_d , propeller revolutions, tracking errors, $n - n_d$, and motor torque, Q_d , commands for the PI-controller versus time.